ISRO Astrosat observations of the Intermediate Polar V1223 Sgr: Study of X-ray pulsations and energy spectrum using LAXPC and SXT

by

Jatan Mehta

Under the guidance of

Dr. Jayashree Roy

(Research Associate at CBS, Mumbai)

&

Prof. Prahlad C. Agrawal

(NASI Senior Scientist)

Centre for Excellence in Basic Sciences

Mumbai, India

December 2017.

Acknowledgements

I would like to express my gratitude and thanks to my guide Dr. Jayashree Roy for giving me the opportunity to work on this project, and to Prof. P. C. Agrawal for his excellent guidance. The constant support of Dr. Jayshree Roy with the analysis has made this work possible. The experience of Prof. P. C. Agrawal has been insightful at every step along the way. Working on this project has been a wonderful learning experience. A ton of gratitude also goes to my parents for being supportive the entire time.

Abstract

We report X-ray analysis findings from the Astrosat satellite data on the Intermediate Polar V1223 Sgr. The data from LAXPC and SXT instruments onboard Astrosat have been used for hard X-ray and soft X-ray analysis respectively. We present timing analysis of the source including energy dependent results. We also report the spin period and modulation in the light curves across the entire energy range of both the instruments. Further, we present spectral analysis of the source for the 3-80 keV range of the LAXPC detector and compare our findings to published literature.

Table of Contents

List of Figures

List of Tables

1. Astrosat space telescope

Astrosat is India's first dedicated multi-wavelength space observatory, launched on an ISRO's PSLV on September, 2015. Put into a 650-km near-equatorial Earth orbit, the expected operating lifetime of the satellite is > 5 years. The five instruments onboard cover the visible (320-530 nm), near UV (180-300 nm), far UV (130-180 nm), soft X-ray (0.3-8 keV and 2-10 keV) and hard X-ray (3-80 keV and 10-150 keV) regions of the electromagnetic spectrum. [1]

Mission

The primary goals of Astrosat are: [3]

- Simultaneous multi-wavelength monitoring of intensity variations in a wide range of cosmic sources, including Active Galactic Nuclei (AGNs).
- Detection and study of X-ray transients.
- Sky surveys in the hard X-ray and UV bands.
- Low to moderate resolution broadband spectroscopic studies of X-ray binaries, AGNs, Supernova Remnant (SNRs), Galactic clusters and stellar coronae.
- Studies of pulsations in X-ray pulsars.
- Studies of periodic and non-periodic variability in X-ray binaries.
- Quasi-Periodic Oscillations (QPOs) and other variations in X-ray binaries.

Ability to study a cosmic source simultaneously in several spectral regions can probe origin of radiation in different spectral regions, their emission regions and processes governing them.

Payloads

The scientific payload has a mass of 1513 kg and contains 6 instruments: [2]

- The **UltraViolet Imaging Telescope (UVIT)** covers the UV and the optical band, performing simultaneous imaging in the 130-180 nm, 180-300 nm, and 320-530 nm bands respectively.
- The **Soft X-ray imaging Telescope (SXT)** employs focusing optics and a deep depletion CCD camera (similar to Swift XRT) at the focal plane to perform X-ray imaging in the 0.3-8 keV band.
- The **3 LAXPC Instruments** cover X-ray timing and low-resolution spectral studies over a broad energy band (3-80 keV). Each Large Area X-ray Proportional Counter (LAXPC) is a multi-wire-multi-layer configuration and have a Field of View of 1°×1°.

- The **Cadmium Zinc Telluride Imager (CZTI)** is a hard X-ray imager consisting of a Pixelated Cadmium-Zinc-Telluride detector array of 500 cm^2 effective area and an energy range from 10-150 keV.
- The **Scanning Sky Monitor (SSM)** consists of 3 position sensitive proportional counters, each with a one-dimensional coded mask (similar to NASA's RXTE). The assembly is placed on a rotating platform to scan the available sky once every six hours in order to locate transient X-ray sources.
- The **Charged Particle Monitor (CPM)** controls the operation of the LAXPCs, SXT and SSM. Even though the orbital inclination of the satellite is $\leq 8°$, in about 2/3 of the orbits, it spends 15-20 minutes in the South Atlantic Anomaly (SAA) region which has high fluxes of low energy protons and electrons. Data from CPM is used to cut-off/lower the high voltage during that time to prevent damage to the detectors as well as to minimize ageing of the proportional counters.

A ”bus” platform connects all the main systems including the battery, computer, antennas, solar arrays, payload instruments and communication equipment. The two solar panel arrays of Astrosat generate about 1600 W power. Two lithium ion batteries (connected to the bus system for charging) supply power to the spacecraft when sunlight is not falling on the solar panels.

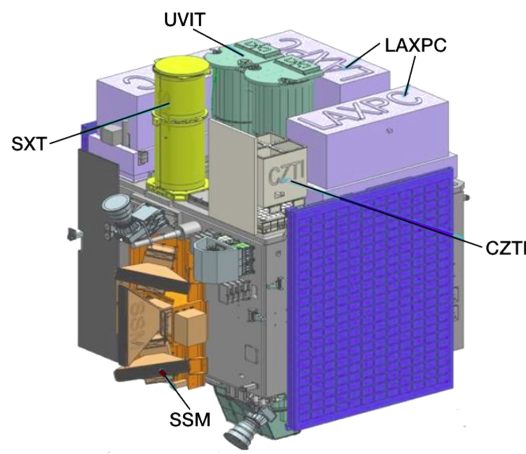

Fig 1: Schematic showing Astrosat detectors [1]

The Attitude and Orbit Control System (AOCS) consists of a host of sun and star sensors, magnetometers as well as sensitive gyroscopes to properly orient the spacecraft and target a source with a pointing accuracy of 0.05°. [2]

2. LAXPC

Introduction

The 3 LAXPC instruments are low-resolution, broadband spectroscopy proportional counters with a large collection area, each with the following characteristics: [4]

X-ray detection volume	100 cm long x 36 cm wide x 15 cm deep
Number of Anode cells	60, arranged in 5 layers, each with 12 Anode cells
Size of each Anode cell	3 cm wide x 3 cm deep x 100 cm long
X-ray entrance window	50 μm thick aluminized Mylar
Anode wire	37 μm diameter gold coated stainless steel
Ground plane cathode wires	50 μm diameter Beryllium-copper wires
Detector gas	90% Xenon + 10% Methane at a pressure of 1520 torr (~2 atmospheres)
Dead time	43 μsec
Field of View	∼1° x 1°
Energy range	3-80 keV
Typical energy resolution	∼12% FWHM at 22 keV
Effective area in 3-15 keV	∼6000cm^2
Effective area in 33-60 keV	∼5000cm^2
Total Effective Area of 3 LAXPC Detectors	~ 8000cm^2in 5-20 keV

Table 1: LAXPC characteristics

Working

Each LAXPC detector consists of the following major parts:

1. Detector, the detector housing and its backplate
2. Collimator (Window support and Field of view collimators)
3. On-board gas purification unit with solenoid valves and plumbing

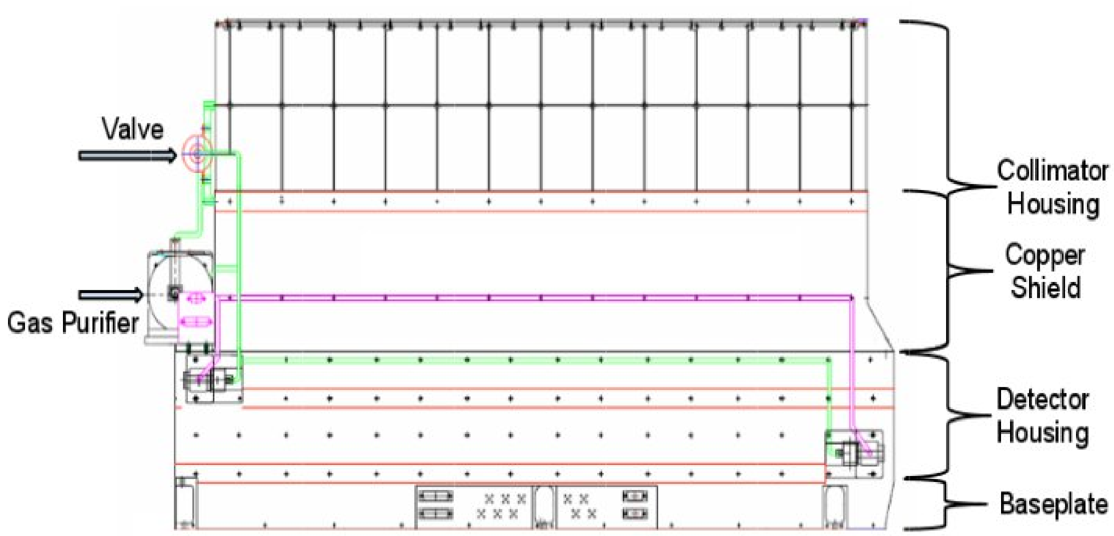

Fig 2: Schematic diagram of a LAXPC detector [4]

Each LAXPC units has its own independent front-end electronics, HV supply and signal processing electronics. The data from all the LAXPCs are independently acquired preserving the identity of each unit. Three independent and modular electronics systems for three LAXPC detectors ensure high reliability and adequate safety measures against single-point failures. Each of the LAXPC detectors has an onboard gas purification system. This system will be operated as and when required to purify the gas filled in the detector. [5]

Only single events originating from one of the 5 X-ray detecting anode layers (except the simultaneous signals that come from K-fluorescent X-ray) that have energy in 3-80 keV, not coincident with any veto signal, are processed for pulse height analysis. Pulse height of each valid X-ray event is analysed by a 1024 channel analyser and also time tagged. [5]

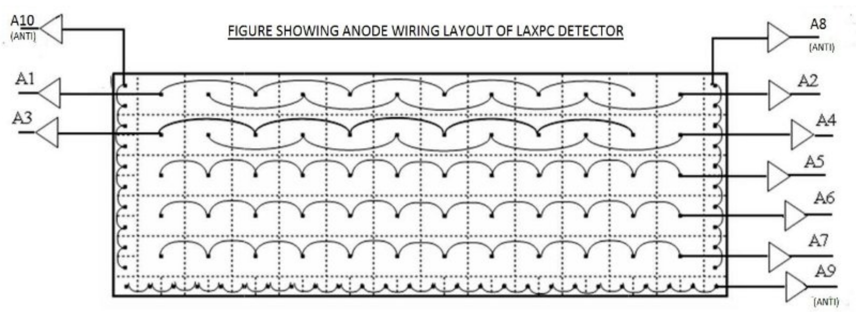

Fig 3: LAXPC anode configuration, mutual anticoincidence and veto scheme. [4]

The detection efficiency of LAXPC is >50% above 30 keV. It provides the largest effective area in 3-80 keV range among all global satellite missions flown so far and will remain so for the next 5-10 years. The LAXPC instrument is best suited for X-ray timing and spectral studies ranging from as short as few milliseconds (for bright sources) up to few hundreds of seconds across its entire energy range. The LAXPC can also study celestial objects that undergo sudden outbursts in the order of tens of microseconds.

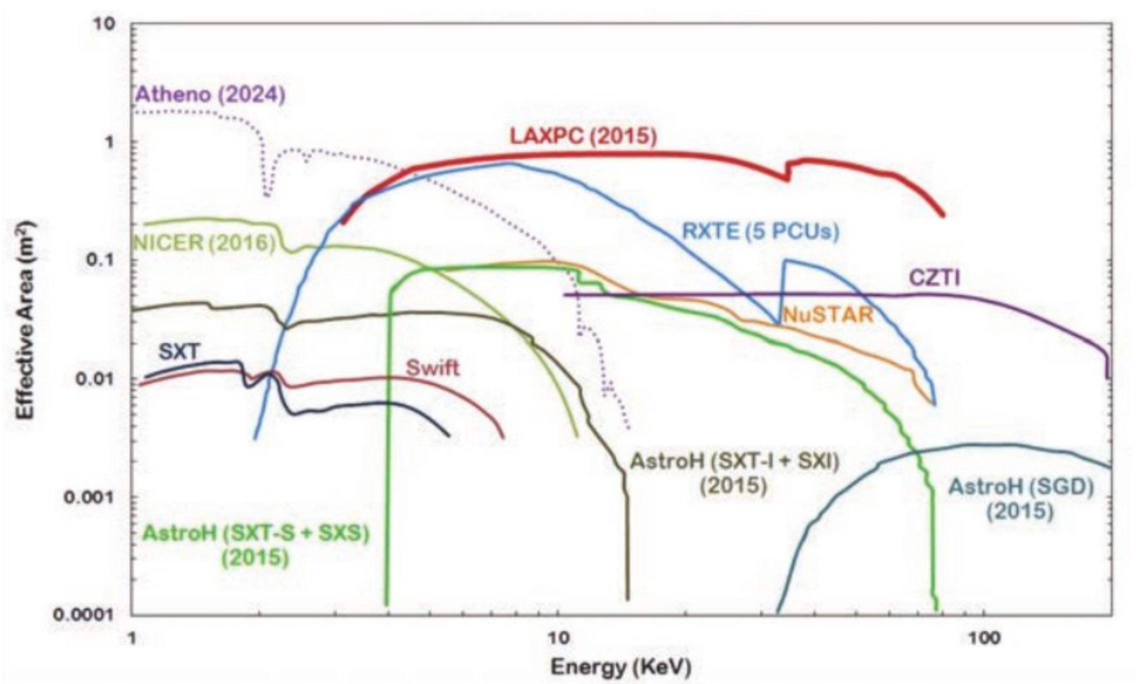

Fig 4: Comparison of LAXPC's effective area with International X-ray missions. [1]

3. SXT

SXT consists of a set of coaxial and confocal shells of conical mirrors approximating paraboloidal and hyperboloidal shapes, arranged behind each other in a geometrical arrangement known as approximate Wolter I optics. X-rays are first reflected by an internally reflecting paraboloidal (1α) mirror and then reflected to the prime focus of the telescope by the internally reflecting hyperboloid (3α) mirror. Nesting of Wolter I shells is incorporated to improve the effective area. [6]

The focal length of the telescope is 2m. Each of the 100 mm length mirror is made of ~0.2 mm aluminum with a replicated gold surface on the reflecting side (similar to Suzaku). The radii of the outermost shell & innermost shell are 130 mm & 65 mm respectively. The smoothness of the mirrors are ~7-10 A° (FWHM).

X-rays are focused on a CCD housed in a Focal Plane Camera Assembly (FPCA). A thermal baffle is placed above the optics and a deployable door is attached at the top of the thermal baffle. All elements of the SXT are joined together by three tubes of CFRP (Composite Fiber Reinforced Plastic). [6]

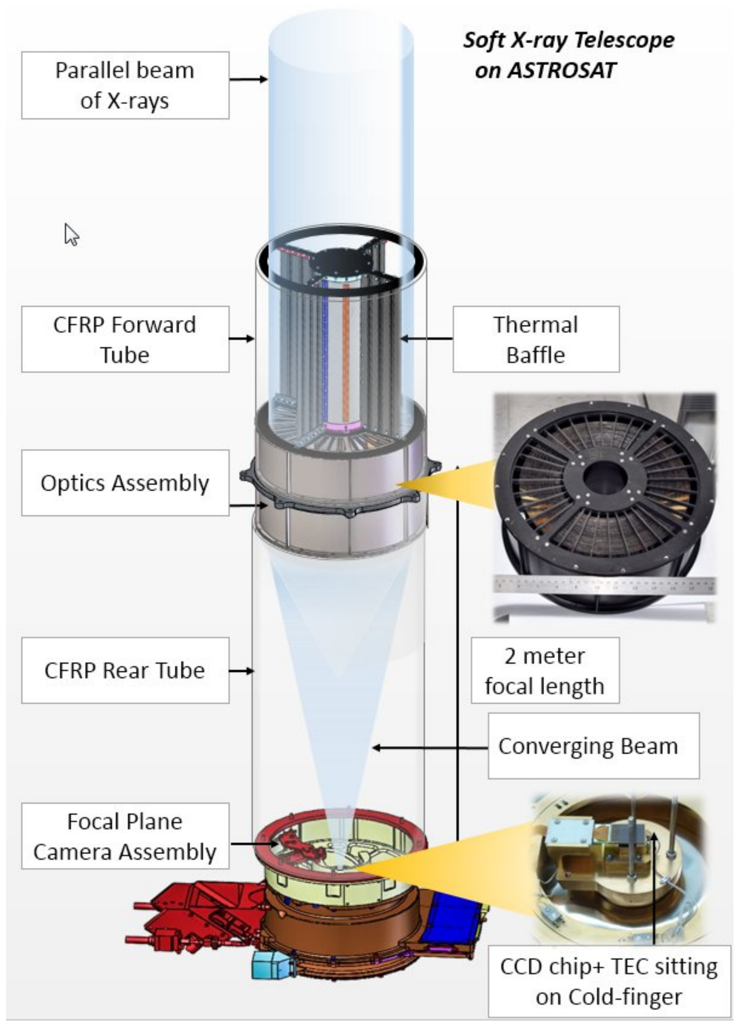

Fig 5: Schematic of SXT showing all its main parts [6]

The detection characteristics of the SXT are as follows: [2]

Energy range	0.3-8 keV
Geometric area	~250 cm^2
Effective area	~128cm^2@1.5 keV, ~22cm^2@6 keV
Field of View (FWHM)	~40’ diameter
Energy Resolution	~5-6% @1.5 keV, ~2.5% @6 keV
Angular Resolution	~2 arc-min
Time resolution	2.4 s, 278 ms

Table 2: SXT characteristics

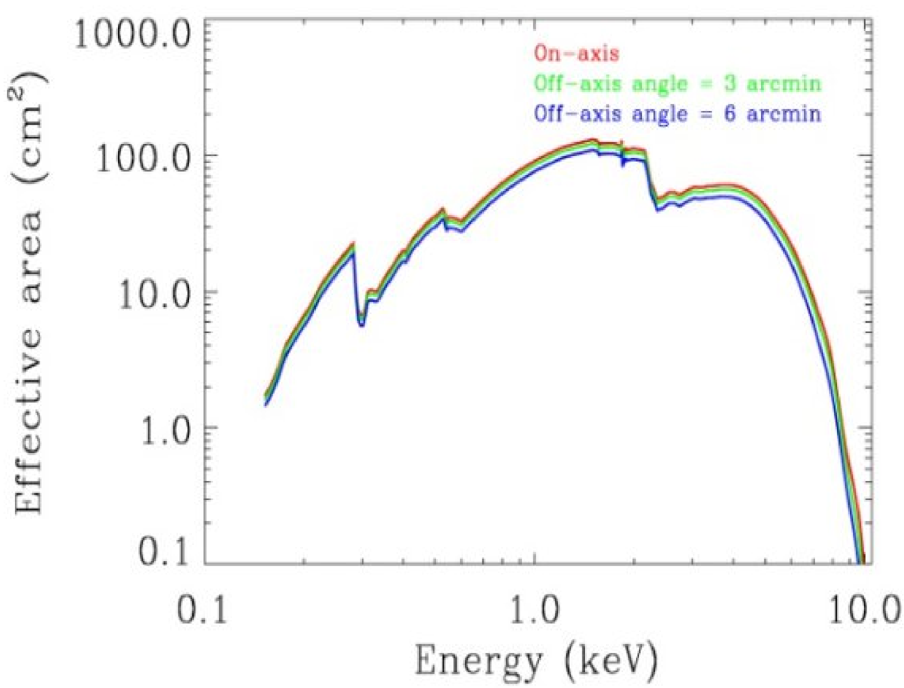

Fig 6: Effective Area of the SXT [6]

4. X-ray Binaries (XRBs)

Introduction

X-ray Binaries are a class of binary stars that are luminous in X-rays, produced by accreting matter on a compact primary (white dwarf/neutron star/black hole) from the secondary normal star. The accreting matter does not hit the compact star directly as it possesses some angular momentum and spirals around the compact star forming the accretion disc in this process.The accretion of matter onto the surface of a compact object releases enormous amount of gravitational energy in the form of X-rays. [7]

Mechanisms for production of X-rays from hot gases:

- **Thermal Bremsstrahlung:** When electrons in an ionized gas of ~10^5K pass close to positive ions, the deceleration causes them to radiate photons (predominantly X-rays) at these temperatures.
- **Synchrotron Radiation:** Electrons accelerated under the influence of a strong magnetic field emit electromagnetic radiation known as synchrotron radiation. The frequency of the radiation depends on the electron energy, the magnetic field strength B, and the direction of motion relative to the field.
- **Inverse Compton Scattering:** A high energy electron colliding with photons of lower energy results in the scattered photon having high energy due to momentum transfer. This process is called Inverse Compton Scattering.
- **Blackbody Radiaion:** The spectrum radiated by the blackbody exhibits peak emission at an energy dependent only on temperature T. At surface temperatures of $T \geq 10^6$ K, X-rays dominate the spectrum.

Classification of X-ray Binaries:

High-mass X-ray Binaries (HMXBs) have a massive O/B type donor star. Accretion is powered either by powerful stellar winds or Roche lobe overflow from donor star onto the compact object.
Low-mass X-ray Binaries (LMXBs) have a K/M type donor star. Mass transfer is via Roche lobe overflow where the matter gets accreted onto the compact object through the inner Lagrangian points. X-rays bursts are commonly seen in LMXBs.

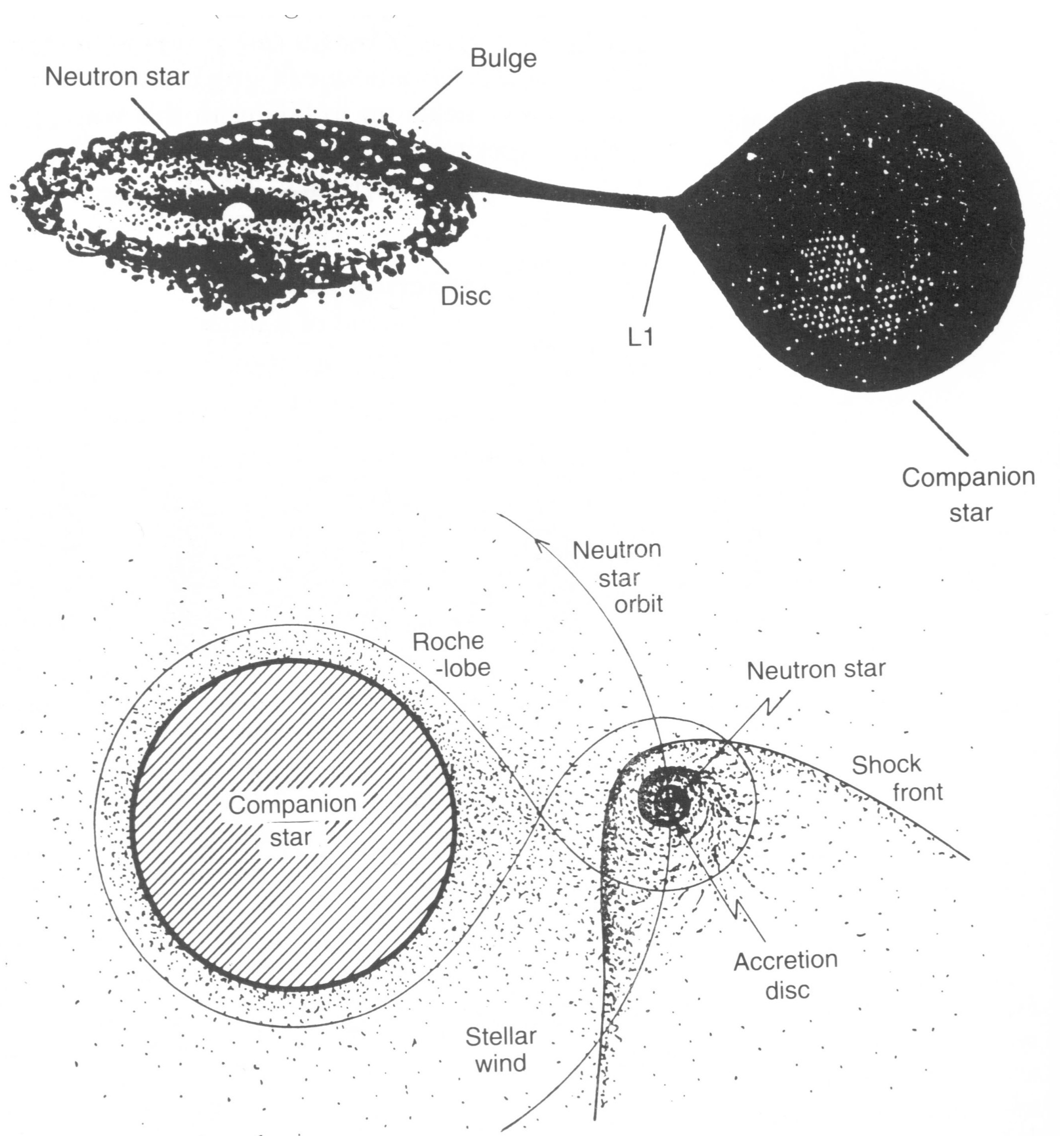

Fig 7: Schematic diagram representing LMXBs and HMXBs [8]

Why are XRBs important?

- Access to exotic endpoints of stellar evolution
- Properties of accretion discs on accessible timescales
- Micro-scale analogues of AGNs (e.g. microquasars, ULXs)
- Probe physical processes close to NS surface or BH event horizon
- Binaries: Mass/size constraints and measurements of their fundamental properties

Low-mass X-ray Binaries (LMXBs)

LMXBs usually have a soft X-ray spectra ($kT < \sim 15$ keV), are known to have frequent X-ray bursts and have faint optical partners. Mostly found in the Galactic Bulge and Globular clusters, their known orbital periods (P) fall under the following:

- $P < 1$ hr: Degenerate stars
- 3 hrs $< P < \sim 10$ hrs: Main-Sequence stars

A typical low-mass X-ray binary emits almost all of its radiation in X-rays and < 1% in visible, making them among the brightest objects in the X-ray sky, but relatively faint in visible light. A bright part of the system is the accretion disk around the compact object.

Cataclysmic variable stars (CV) are a type of LXMB, which irregularly increase in brightness by a large factor, then drop back down to a quiescent state. The large outbursts are associated with Novae, and the variables in which the White Dwarf star has a significant magnetic field are Polars.

5. Intermediate Polars

An Intermediate Polar (IP) is a part of a LMXB, similar to other Cataclysmic Variable (CV) stars except that the inner accretion disk is truncated by the magnetic field of the White Dwarf. In that inner region, the gas in the disk begins to travel along the white dwarf's magnetic field lines, forming curved sheets of luminous material called accretion curtains. Disk material passes through the curtains and then accretes onto the white dwarf near one of its magnetic poles. The magnetic field of an Intermediate Polar is typically 100-1000 T, in between non-magnetic CVs and highly magnetic ones. [9]

Intermediate polar systems are strong X-ray emitters. The X-rays are generated by high velocity particles from the accretion stream forming a shock as they fall onto the surface of the white dwarf star. As particles decelerate and cool before hitting the white dwarf surface, bremsstrahlung X-rays are produced and may subsequently be absorbed by gas surrounding the shock region. At the intersection of the accretion stream and the surface of the white dwarf, a hot spot is produced at both the magnetic poles.

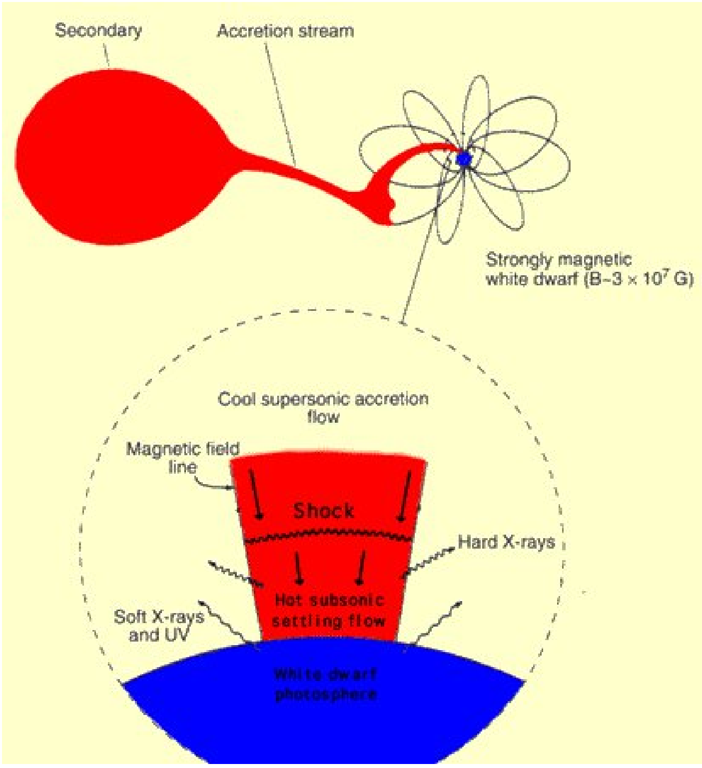

Fig 8: Origin of X-ray emission in IPs

The infalling material encounters a shock front as the density increases before hitting the star surface, converting the kinetic energy to thermal energy. The falling material radiates using cyclotron emission (in radio/IR for IPs) and optically thin thermal bremsstrahlung radiation (hard X-rays), while the heated poles radiate in UV and soft X-rays. The light curve of an IP shows multiple periodicities: Spin, Orbital and Sideband period. [9]

6. Data analysis for source V1223 Sgr

Astrosat data for the Intermediate Polar V1223 Sgr (d=527 pc and i=24°) [10] is studied and discussed here. The data of the source is obtained from the LAXPC and SXT instruments for the time: 11-08-2016 to 12-08-2016 (MJD: 57611 to 57612). The subsequent Astrosat orbits covered are 4715, 4716, 4717, 4719, 472, 4721, 4722, 4723, 4724 & 4727. The software used for the data analysis (timing analysis, periodicity, spectra) is HEASOFT by NASA and a set of tools developed for Astrosat (e.g. lxplc software).

Timing analysis: All the light curves (intensity variation with time) in different energy bands were extracted in the FITS file format and binning of 1s was used throughout. All the subsequent LAXPC data shown is from files that are barycenter corrected and background corrected. The background for both LAXPC and SXT have been taken during the same time period.

Timing analysis has been done dividing the data into different energy bands of 3-6, 6-10, 10-20, 20-40, 40-60 and 60-80 keV respectively. The Channel and Layer (L) selection is as follows:

Energy range (Layer selection)	Lxp 1	Lxp 2	Lxp 3
3-6 (L1 - L2)	24-50	24-44	18-42
6-10 (L1 - L2)	50-84	44-76	42-76
10-20 (L1 - L2)	84-168	76-148	76-158
20-40 (L1 - L7)	168-324	148-268	158-306
40-60 (L1 - L7)	324-466	268-384	306-450
60-80 (L1 - L7)	466-594	384-476	450-584

Spin period: For the spin period, the heasoft module efsearch is used to find the spin period of the White Dwarf using epoch folding. Given an approximate known period, efsearch folds data over certain range of periods around this value and gives an accurate period. We used the default epoch (17611) for the plots and a Gaussian fit is made to the peak to obtain the error in the best period obtained from the analysis, where the width of the fitted peak is the error. For

LAXPC data, from all the three detectors is merged for better statistics. We ran efsearch with a resolution of 0.1 s and 8 phasebins per period.

Periodicity in light curves: The heasoft package efold is used for finding periodicities in light curves. The spin-period folded and binned X-ray light curves for the different energy ranges shows the periodicity in light curves in the data. For LAXPC, data from all the three detectors is merged for better statistics. The epoch is 17611.642849444015 and there are 32 phasebins per period.

Spectral Analysis: Broadband Spectral analysis was done on the LAXPC 1 data to cover the full energy range of 3-80 keV since for LAXPC 2 & 3, the background dominates the source above 50 keV. The files used for spectral fitting of LAXPC 1 and SXT are as follows:

1. LAXPC:

Data: lxp1level2.spec
Backgrnd: lxp1level2back.spec
Response: lx10cshp04v1.0.rmf

2. SXT

Data: merged_cl_3.pha
Backgrnd: Sky8nBSCombpha_spec.pha
Response:
sxt_pc_matrix_g0to12_en6.75_cti0.7_0.2_dd23_29_ff52_46_etestapb11j_Na2.5_S1.1_Lf217.5_Ls0.75_loss2.3_thr150.rmf
Arf: Astrosat_120arcsec_rad_uol.arf

Data and Background are from the same month and an appropriate response matrix is used.

7. Timing Analysis

The 3-80 keV light curves for all LAXPCs are as follows:

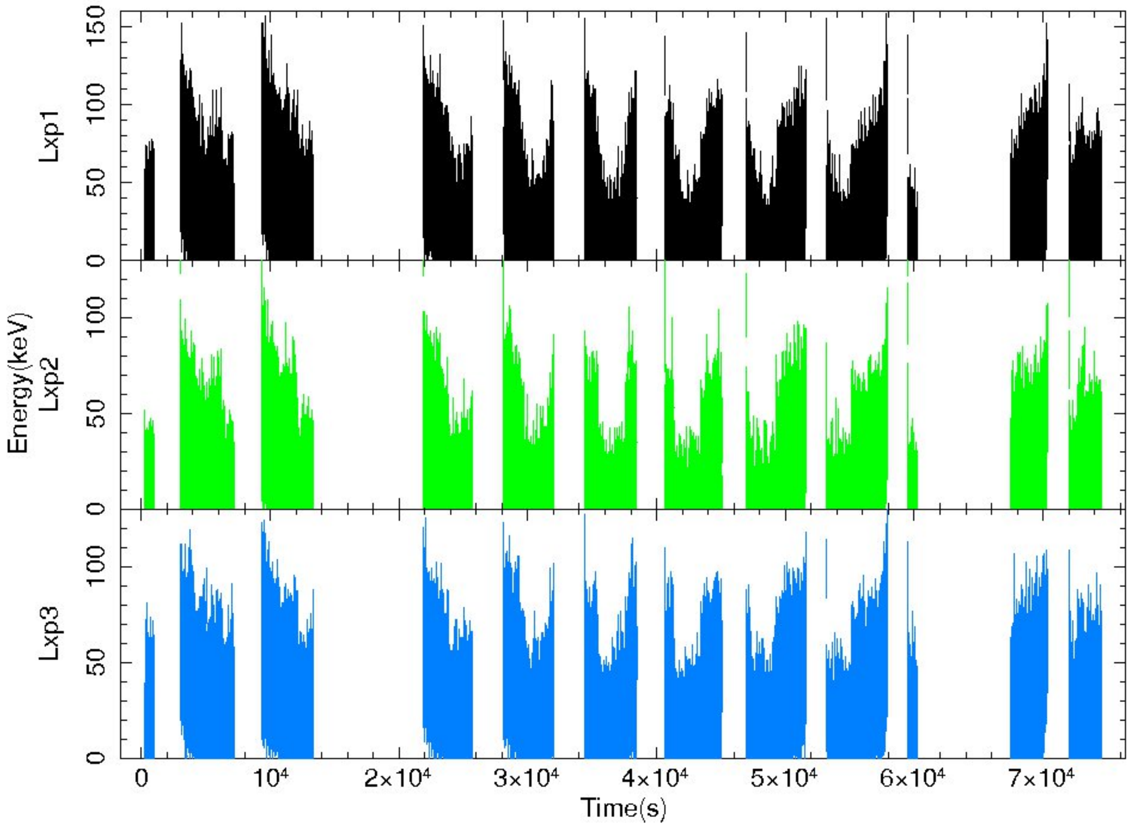

Fig 9: 3-80 keV light curves for LAXPC 1,2 & 3

The individual light curves for each energy range, per LAXPC are as follows:

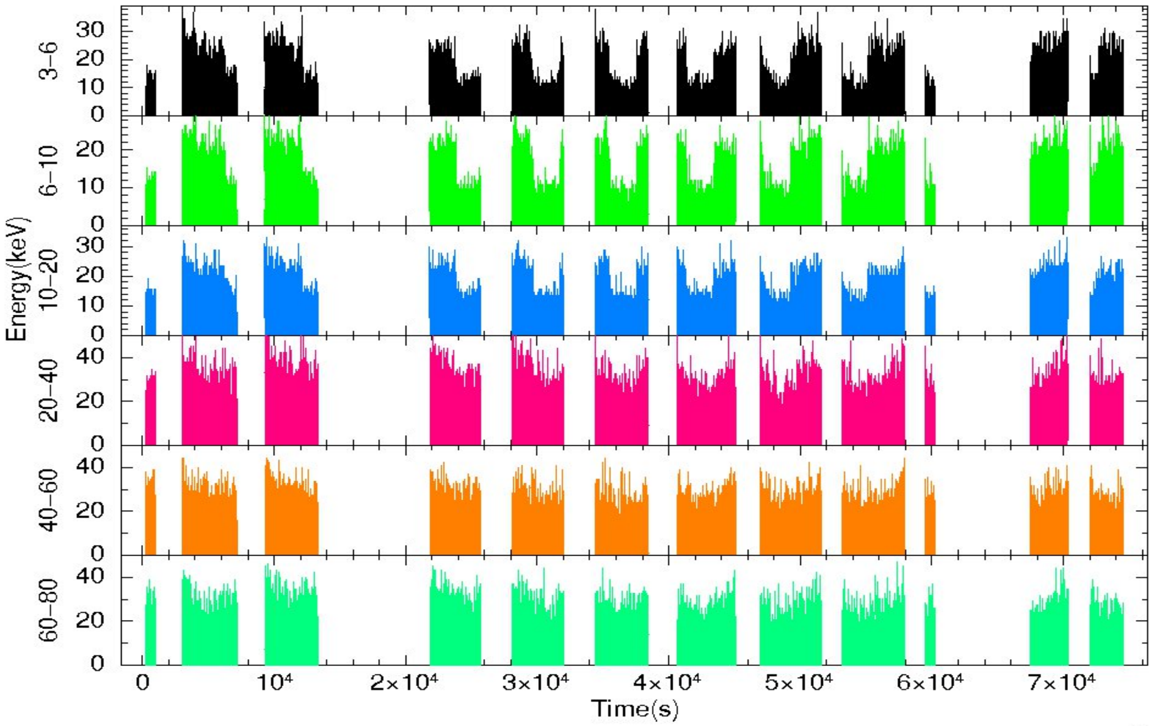

Fig 10.1: Energy dependent light curves for LAXPC 1

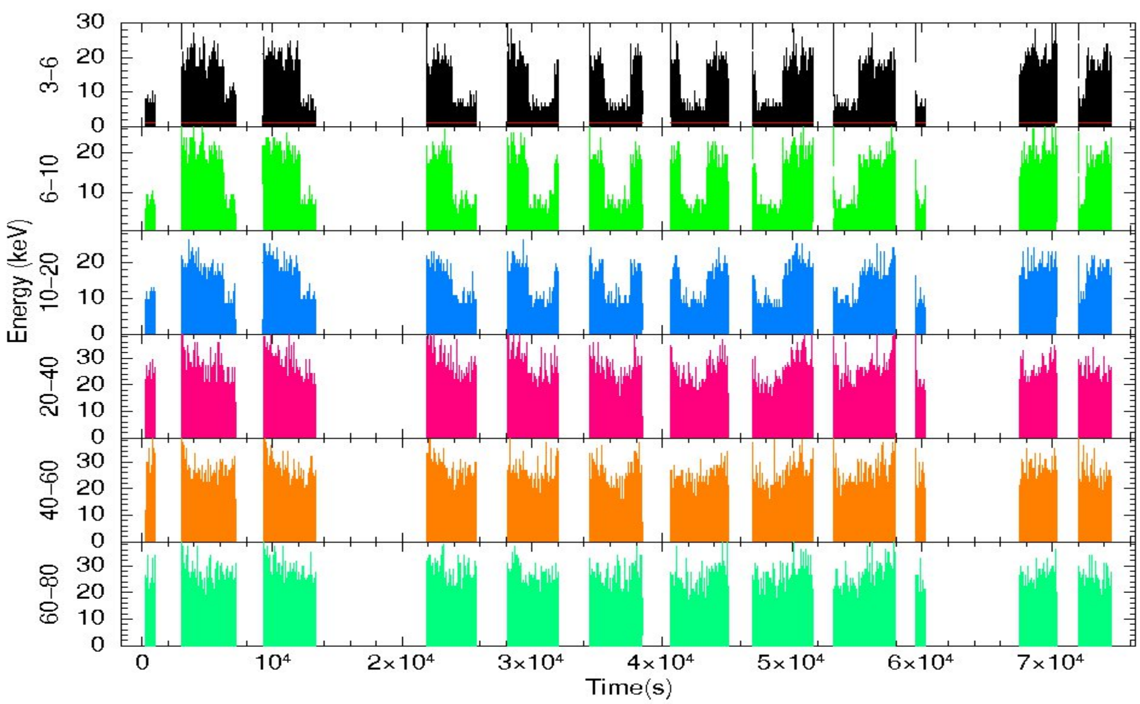

Fig 10.2: Energy dependent light curves for LAXPC 2

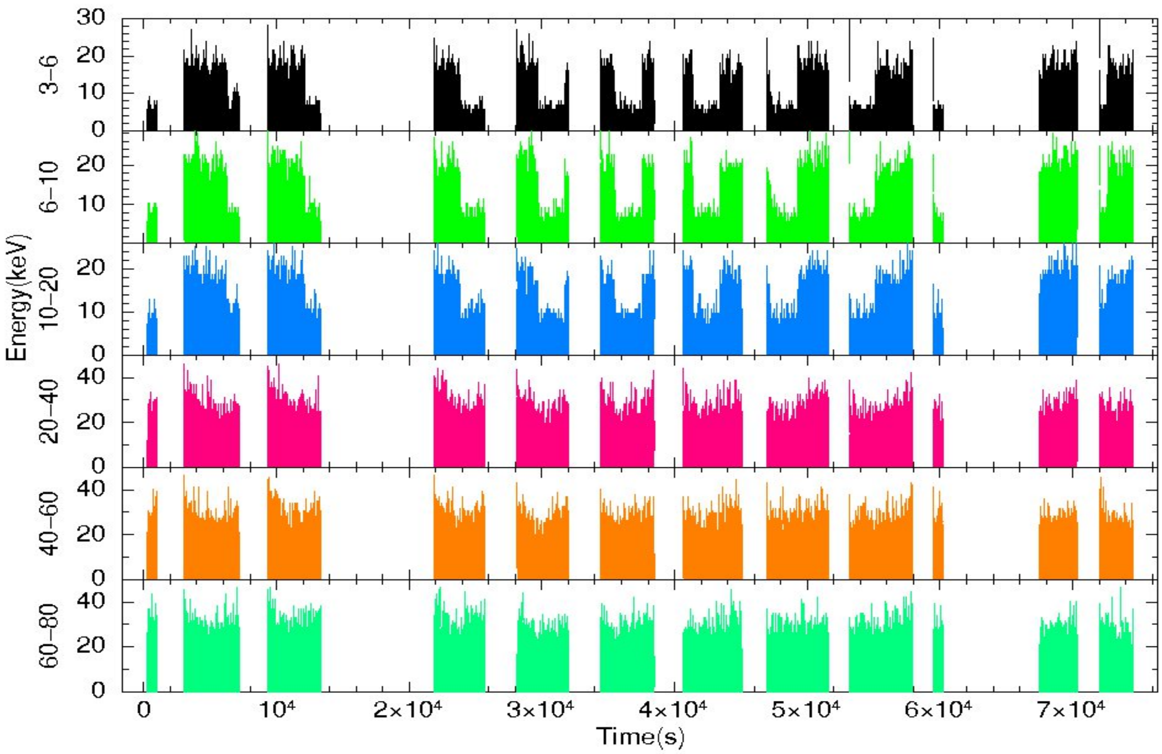

Fig 10.3: Energy dependent light curves for LAXPC 3

The data gaps in the light curves are due the SAA passages in the orbit of Astrosat, where the CPM cuts off the detector voltage to prevent radiation damage. The dips in the light curves where the count rate abruptly drops is due to the Earth occultation of the satellite. The sharp lows are the partial eclipses of the source by its companion. There is a variation in intensity (at the time scale of ~10^4 s) associated with the orbital motion of the binary system.

The count rate for each LAXPC per energy range is tabulated below:

Energy range (keV)	**LAXPC**	**Source (Error +-)**	**Background (+-)**	**Net (+-)**
3-6	**lxp1**	18.32 (0.02)	13.54 (0.02)	6.35 (0.03)
	lxp2	7.74 (0.01)	3.88 (0.01)	4.93 (0.02)
	lxp3	7.23 (0.01)	3.69 (0.01)	4.41 (0.02)
6-10	**lxp1**	13.19 (0.02)	9.04 (0.02)	5.61 (0.03)
	lxp2	8.47 (0.02)	4.68 (0.02)	4.83 (0.03)
	lxp3	8.46 (0.01)	4.23 (0.01)	5.39 (0.02)
10-20	**lxp1**	16.73 (0.02)	12.38 (0.02)	6.12 (0.03)
	lxp2	10.66 (0.02)	7.7 (0.02)	4.44 (0.03)
	lxp3	10.36 (0.02)	6.94 (0.01)	4.77 (0.02)
20-40	**lxp1**	54.4 (0.04)	50.31 (0.04)	9.06 (0.05)
	lxp2	37.34 (0.03)	36.17 (0.03)	6.71 (0.05)
	lxp3	34.69 (0.03)	29.94 (0.03)	7.91 (0.04)
40-60	**lxp1**	51.6 (0.04)	49.69 (0.04)	7.68 (0.05)
	lxp2	41.15 (0.03)	41.12 (0.03)	6.51 (0.05)
	lxp3	39.68 (0.03)	34.71 (0.03)	8.27 (0.04)
60-80	**lxp1**	50.3 (0.04)	49.2 (0.04)	7.69 (0.05)
	lxp2	39.51 (0.03)	39.41 (0.03)	6.67 (0.05)
	lxp3	41.69 (0.03)	37.27 (0.03)	8.45 (0.04)

Table 3: Count rates (source, background and net) per energy range for each LAXPC

8. Spin Period

We ran efsearch with a resolution of 0.1 s and 8 phasebins per period and we got the spin-periods for different energy bands for the LAXPC & the SXT detectors as tabulated below:

Energy range (keV)	LAXPC 3-80	LAXPC 3-6	LAXPC 6-10	LAXPC 10-20	SXT 0.3-8
Spin Period (s)	746 (Error = 2.6)	745.7 (2.7)	745.8 (2.7)	745.2 (3.2)	744.9 (4.1)

Table 4: Spin periods obtained for LAXPC and SXT

The spin period thus obtained are consistent within different energy bands (including the errors) and with earlier reported values by other X-ray observatories & optical data too. A proper Gaussian fit could not be obtained for the other energy ranges.

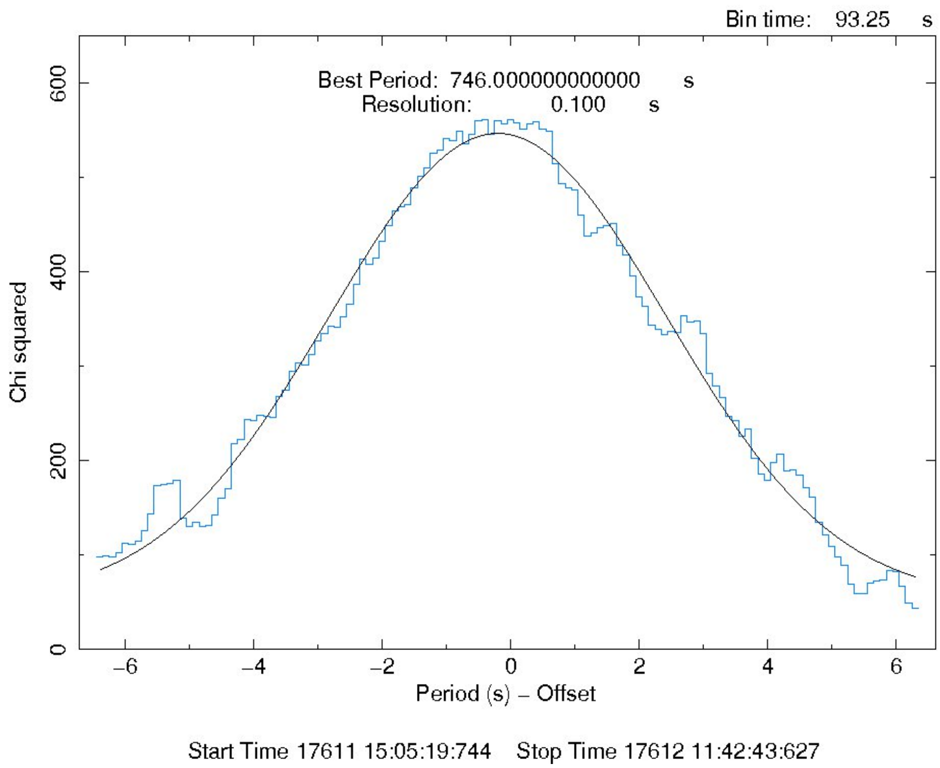

Fig 11: Spin Period for 3-80 keV data (LAXPC) using efsearch

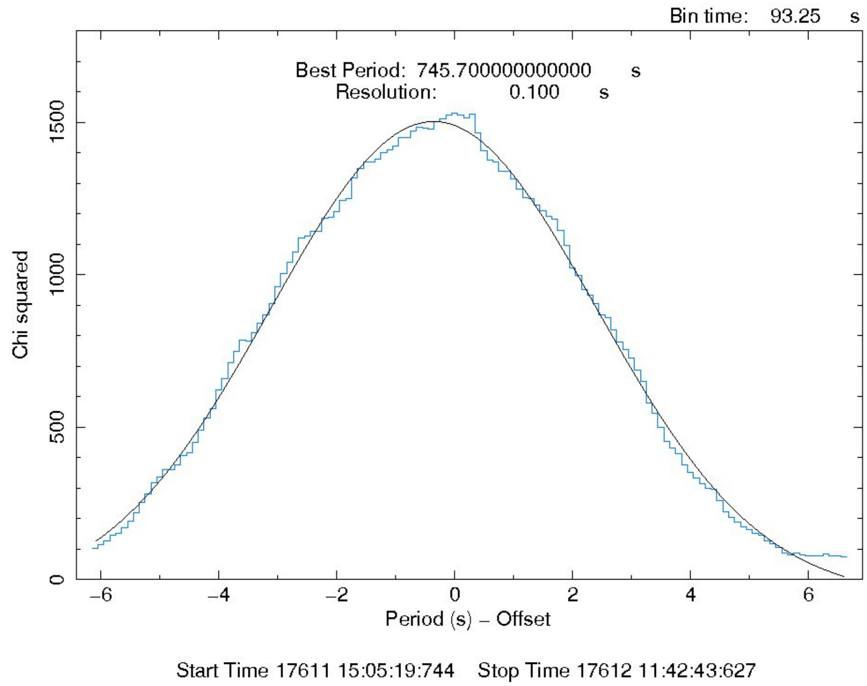

Fig 12.1: Spin Period for 3-6 keV data (LAXPC) using efsearch

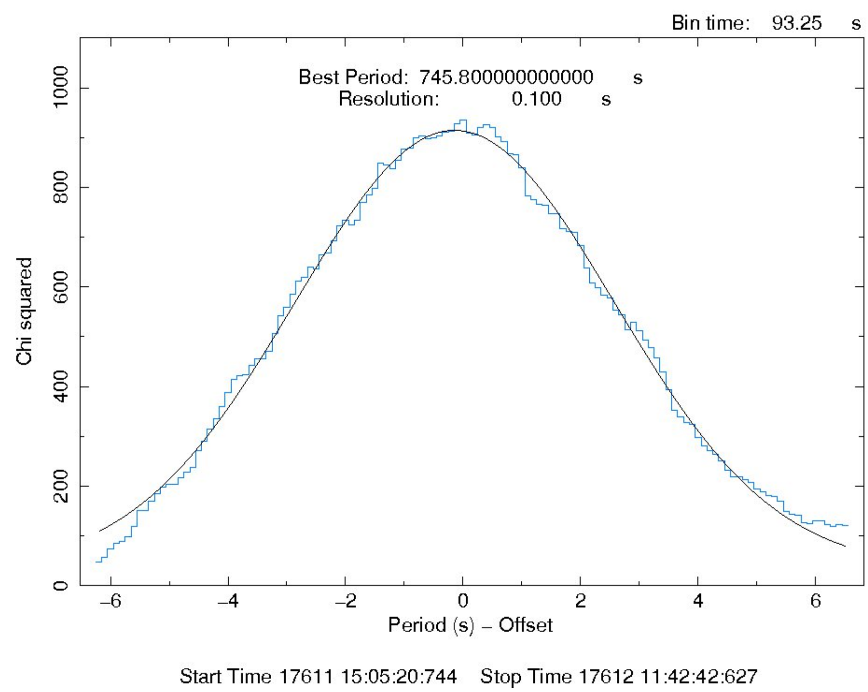

Fig 12.2: Spin Period for 6-10 keV data (LAXPC) using efsearch

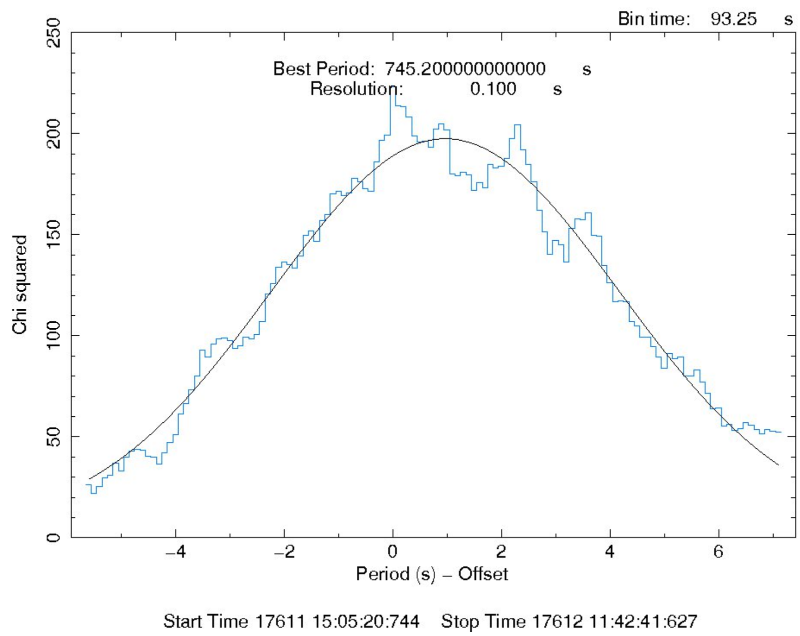

Fig 12.3: Spin Period for 10-20 keV data (LAXPC) using efsearch

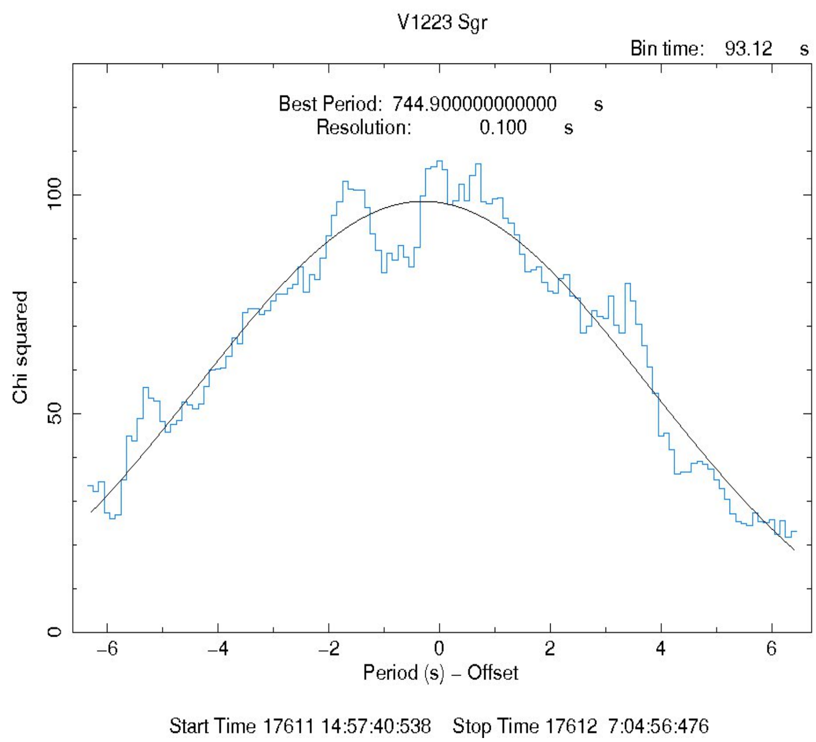

Fig 13: Spin Period for 0.3-8 keV data (SXT) using efsearch

9. Periodicity in Light curves

The following efold results (pulse profile) are attached below: 3-80 keV and energy dependent plots for merged LAXPC 1+2+3 and one for 0.3-8 keV SXT.

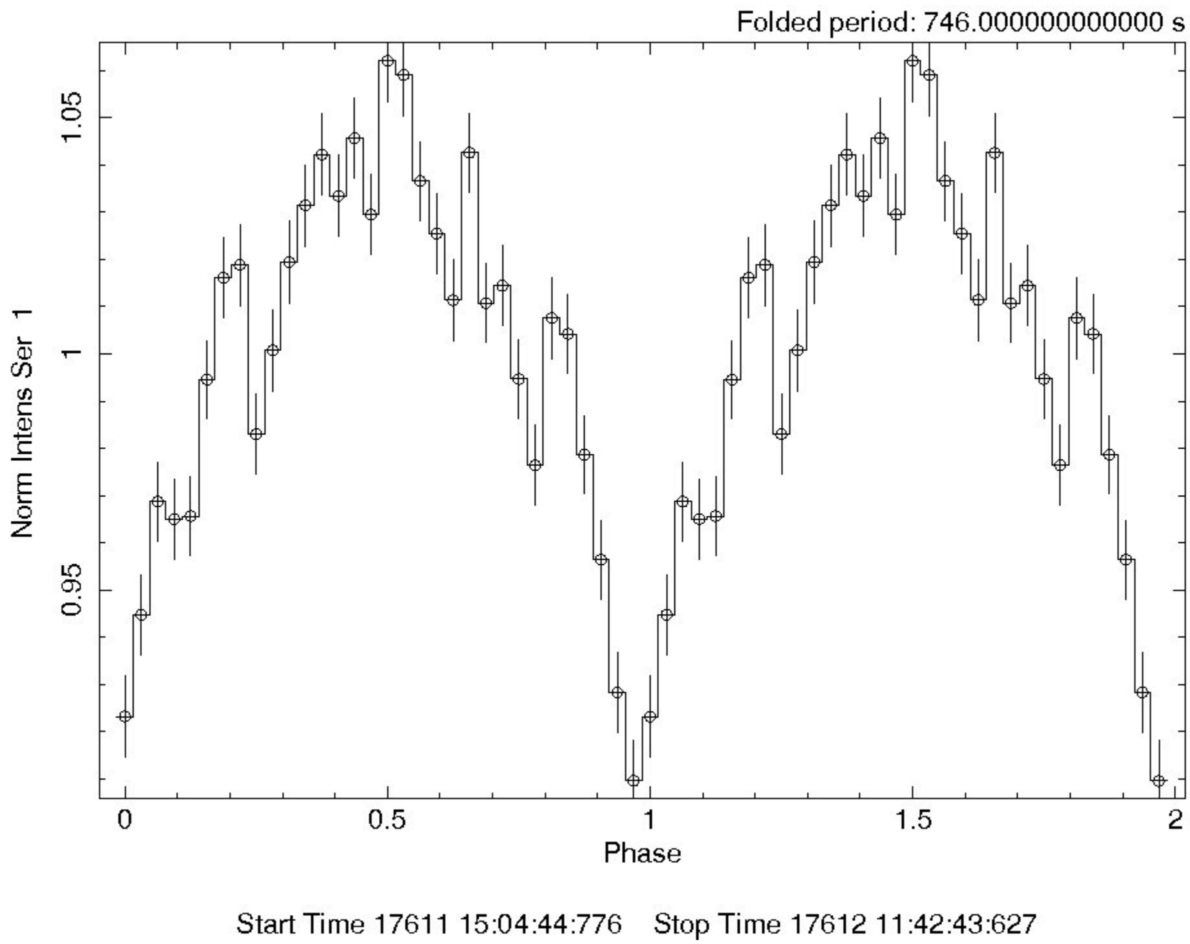

Fig 14: Pulse profile for 3-80 keV data (LAXPC) using efold

The 3-80 keV profiles for LAXPC are almost sinusoidal in nature and a clear modulation is seen at the spin period.

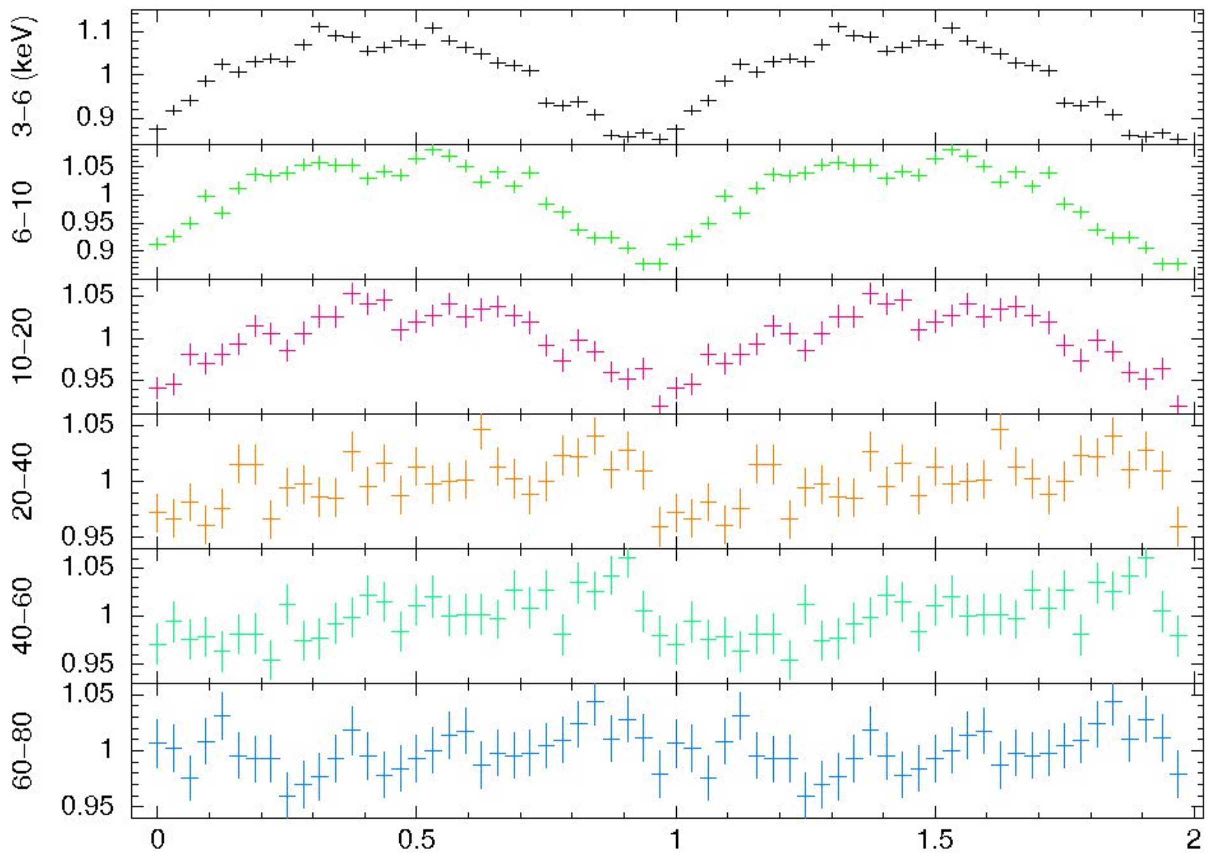

Fig 15: Energy dependent pulse profiles for LAXPC data

They show strong modulation at the spin period. The profile of the folded right curves are almost sinusoidal upto 20 keV. Beyond that, a flat profile stars to appear and is weak and non-sinusoidal, as also seen in the Pulse Fraction tabulated below. The pulse profile for SXT data is similar to the LAXPC ones at lower energy ranges.

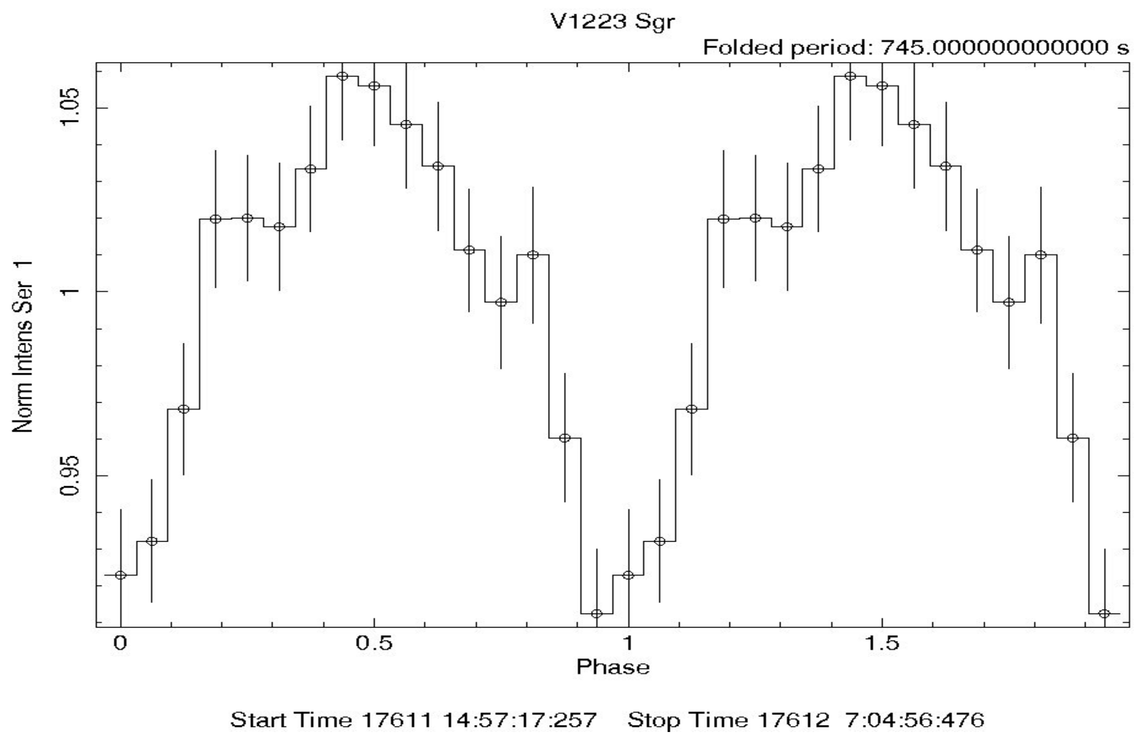

Fig 16: Pulse profile for 0.3-8 keV data (SXT) using efold

Pulse fraction, given by $I_{max} - I_{min} / I_{max} + I_{min}$ used to see modulation was as follows:

Detector	Energy range	Count fraction	Pulse %	Error	Avg counts/s (with error)
Lxp 1+2+3	3-6	0.123	12.3	2.977E-03	16.24 (0.06)
	6-10	0.097	9.7	2.173E-03	15.82 (0.04)
	10-20	0.054	5.4	1.447E-03	15.29 (0.05)
	20-40	0.028	2.8	8.705E-04	23.69 (0.08)
	40-60	0.033	3.3	1.446E-03	22.39 (0.09)
	60-80	0.027	2.7	1.161E-03	22.85 (0.09)
	3-80	0.067	6.7	1.213E-03	49.02 (0.09)
SXT	**0.3-8**	0.073	7.3	3.693E-03	3.47 (0.02)

Table 5: Energy dependent pulse fractions for LAXPC and SXT data

10. Spectral Analysis

For magnetic CVs like V1223 Sgr, simple models consisting of a bremsstrahlung continuum plus iron line emission, with absorption, have been found to adequately describe the hard X-ray spectra. [11]

Here we get a reduced chi-squared of 1.14 for systematic error of 0.02. The base model is taken as absorbed powerlaw (tbabs absorption model and powerlaw base), applied to the entire energy range of 3-80 keV of LAXPC 1. A multi-temperature model is also seen in the spectra. Thermal Bremsstrahlung emission in hard X-rays at ~14 keV is seen as is expected from post-shock temperatures (PST) in LMXBs. Such spectral model should approximately represent emission of the hot plasma in the post-shock region of V1223 Sgr. The best fit temperature of the bremsstrahlung emission denotes the maximal temperature in the post-shock region of the accretion column of the IP. The model diskbb was required to model the soft X-rays coming from the accretion disk at ~7 keV.

Moreover, we see 3 broad-line Gaussian emissions at 6.4 keV, 6.7 keV and 7.0 keV respectively. The 6.4 keV line is the emission of an iron-K(alpha) fluorescence line, which indicates the existence of reflecting cold matter, such as the WD surface and the pre-shock accretion matter. Reflection of hard X-rays from the white dwarf surface could contribute significantly to the observed Fe Kα fluorescence line in intermediate polars. [11] The emission of the He-like (6.7 keV) and H-like (7.0 keV) lines [12] is due to photoionization and collisional ionization/excitation in a hot plasma. Since the hard X-rays from the source is thermal in origin, it is likely that these emission lines are produced through collisional plasma rather than photoionization. This could and should be tested with future Astro-H observations.

For LAXPC 2 & 3, background dominated the source above 50 keV and good fits could not be obtained for them. The reduced chi-squared for both was well above 2 and since the fit parameters were not in agreement with the LAXPC 1 detector, which covered the full energy range and had better data, the fits for LAXPC 2 and 3 are not included here.

The spectral fit and the parameter values for LAXPC 1 are as follows:

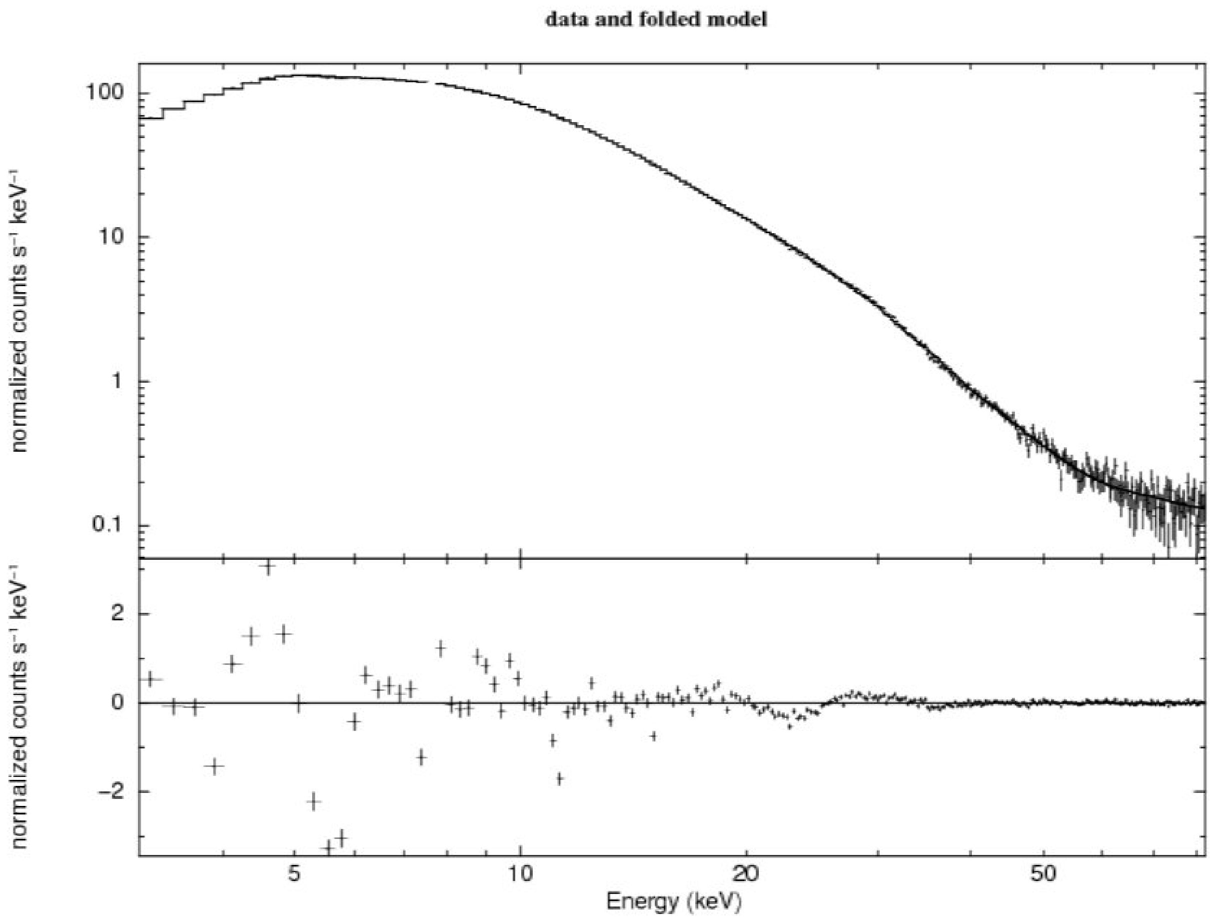

Fig 17: Spectral fitting for 3-80 keV LAXPC 1 data

Models used: TBabs*powerlaw + gaussian + gaussian + bremss + diskbb + gaussian

The reduced chi-squared at systematic errors 0.01 and 0.02 are as follows:

Syst 0.01: Reduced chi-squared = 1.91 for 278 degrees of freedom

Syst 0.02: Reduced chi-squared = **1.14** for 278 degrees of freedom

FIT PARAMETERS:

Par no.	Comp no.	Component	Parameter	Unit	Value	Error range	
1	1	TBabs	nH	10^22	5.00000	frozen	
2	2	powerlaw	PhoIndex		-1.99577	-2.69663	-1.72557
3	2	powerlaw	norm		2.70859E-08	1.2451e-08	2.32582e-07
4	3	gaussian	LineE	keV	6.40269	frozen	
5	3	gaussian	Sigma	keV	2.38771	1.7769	4.5431
6	3	gaussian	norm		7.52556E-02	0.061721	0.148292
7	4	gaussian	LineE	keV	6.70114	frozen	
8	4	gaussian	Sigma	keV	4.45536		
9	4	gaussian	norm		0.167388	0	6.15532
10	5	bremss	kT	keV	13.6910	10.36111	17.8178
11	5	bremss	norm		0.11349	0.095484	0.58022
12	6	diskbb	Tin	keV	7.34649	1.33166	3.1972
13	6	diskbb	norm		0.124634	0	0.251366
14	7	gaussian	LineE	keV	7.00000	frozen	
15	7	gaussian	Sigma	keV	4.40895		
16	7	gaussian	norm		8.43206E-02	0	0.230246

Table 6: Spectral fit parameters for LAXPC 1. All the errors are at the 90% confidence level.

The flux value for 3-80 keV is 1.17^{-8} $ergs/cm^2/s$ which can give the emission measure of the accretion column and luminosity. Since our spectral modeling includes the hard X-ray energy range up to 80 keV, it provides a confident estimation of the post-shock temperature.

An ideal fit could not be obtained for SXT but the components used are similar and two distinct Gaussian lines are seen to peak at 5.97 keV and 6.55 keV. The fit plot and parameters are as follows:

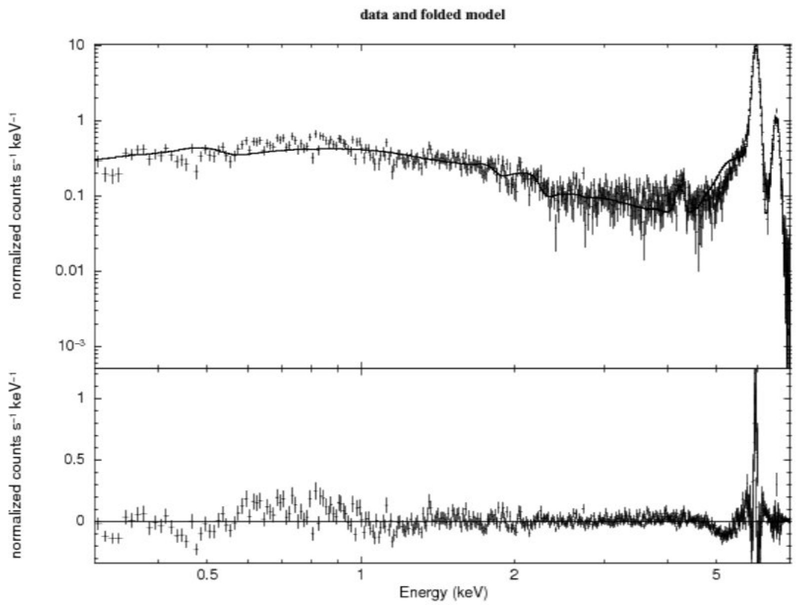

Fig 18: Spectral fitting for 0.3-8 keV SXT data

Models used: TBabs*powerlaw + gaussian + gaussian + diskbb

The reduced chi-squared at systematic errors 0.01 and 0.02 are as follows:

Syst 0.01: Reduced chi-squared = 2.81 for 659 degrees of freedom

Syst 0.02: Reduced chi-squared = **2.72** for 659 degrees of freedom

FIT PARAMETERS:

Par	Comp no	Component	Parameter	Unit	Value	
1	1	TBabs	nH	10^22	5.00000	frozen
2	2	powerlaw	PhoIndex		3.76974	+/- 9.57182E-02
3	2	powerlaw	norm		0.170224	+/- 1.83855E-02
4	3	gaussian	LineE	keV	5.97806	+/- 5.43335E-04
5	3	gaussian	Sigma	keV	3.52676E-02	+/- 8.87511E-04
6	3	gaussian	norm		6.77078E-02	+/- 4.12626E-04
7	4	gaussian	LineE	keV	6.55398	+/- 1.60571E-03
8	4	gaussian	Sigma	keV	4.47762E-02	+/- 2.28286E-03
9	4	gaussian	norm		1.39713E-02	+/- 2.38610E-04
10	5	diskbb	Tin	keV	0.432102	+/- 1.21466E-02
11	5	diskbb	norm		18.3513	+/- 1.97926

Table 7: Spectral fit parameters for SXT. Errors could not be calculated because fit isn't ideal.

An ideal fit could not be obtained for the combined LAXPC-SXT data and the components used are not found similar to the individual fits. The fit plot and parameters are as follows:

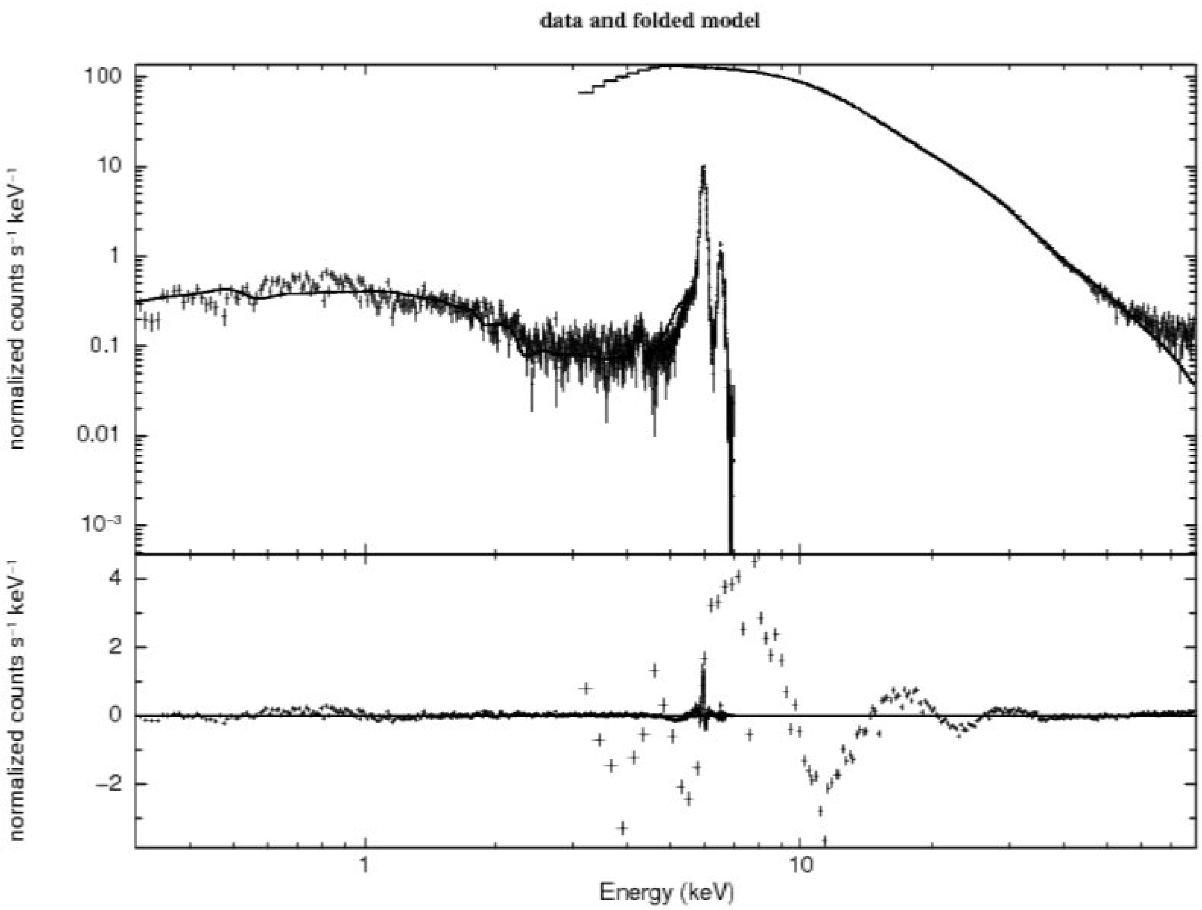

Fig 19: Spectral fitting for combined LAXPC (right) +SXT (left) data

Models used : constant*TBabs*bremss + gaussian + gaussian + mekal + diskbb

The reduced chi-squared at systematic errors 0.01 and 0.02 are as follows:

Syst 0.01: Reduced chi-squared = 3.56 for 934 degrees of freedom

Syst 0.02: Reduced chi-squared = **2.96** for 934 degrees of freedom

FIT PARAMETERS: (PTO)

Par.	Comp.	Component	Parameter	Unit	Value	
			Data group: 1 (SXT)			
1	1	constant	factor		0.531497	+/- 5.22026E+04
2	2	TBabs	nH	10^22	1.60158	+/- 0.405285
3	3	bremss	kT	keV	28.8444	+/- 0.730146
4	3	bremss	norm		1.14277E-02	+/- 1122.42
5	4	gaussian	LineE	keV	5.97838	+/- 5.84636E-04
6	4	gaussian	Sigma	keV	3.61024E-02	+/- 9.32755E-04
7	4	gaussian	norm		6.64398E-02	+/- 4.47976E-04
8	5	gaussian	LineE	keV	6.55368	+/- 1.64038E-03
9	5	gaussian	Sigma	keV	4.26368E-02	+/- 2.40015E-03
10	5	gaussian	norm		1.37832E-02	+/- 2.42902E-04
11	6	mekal	kT	keV	7.57691	+/- 4.15171
12	6	mekal	nH	cm-3	1.00000E+20	frozen
13	6	mekal	Abundanc		0.400000	frozen
14	6	mekal	Redshift		0.0	frozen
15	6	mekal	switch		1	frozen
16	6	mekal	norm		1.06495E-02	+/- 5.41854E-03
17	7	diskbb	Tin	keV	0.309895	+/- 7.30883E-02
18	7	diskbb	norm		24.8976	+/- 9.95222
			Data group: 2 (LAXPC)			
19	1	constant	factor		48.0226	+/- 4.71676E+06
20	2	TBabs	nH	10^22	1.60158	= p2
21	3	bremss	kT	keV	28.8444	= p3
22	3	bremss	norm		1.14277E-02	= p4
23	4	gaussian	LineE	keV	6.00000	frozen
24	4	gaussian	Sigma	keV	4.39047	+/- 2.84703E-02
25	4	gaussian	norm		0.437727	+/- 6.81950E-03
26	5	gaussian	LineE	keV	7.00000	frozen
27	5	gaussian	Sigma	keV	10.9750	+/- 0.104030
28	5	gaussian	norm		0.164043	+/- 5.13238E-03
29	6	mekal	kT	keV	7.57691	= p11
30	6	mekal	nH	cm-3	1.00000E+20	= p12
31	6	mekal	Abundanc		0.400000	= p13
32	6	mekal	Redshift		0.0	= p14
33	6	mekal	switch		1	= p15
34	6	mekal	norm		1.06495E-02	= p16
35	7	diskbb	Tin	keV	0.309895	= p17
36	7	diskbb	norm		24.8976	= p18

Table 8: Spectral fit parameters for combined LAXPC-SXT data. Errors could not be calculated because fit isn't ideal.

Conclusion

The temporal properties of the source V1223 Sgr have been studied for the 3-80 keV energy range, including energy dependent results, all showing variation in intensity related to the orbital period of the system. Additionally, the spin period was found using both LAXPC and SXT to be ~746 s, in agreement with other global missions. The variation of intensity with respect to the obtained spin period is also studied to look for modulations which have been found to be substantial past the 20 keV energy range. A spectral fit for the LAXPC 3-80 keV data was obtained with a reduced chi-squared of 1.14. The spectral analysis allowed us to understand the physical processes going on in the system and calculate the flux of the emission from the accretion column. The mass of the white dwarf star can further be determined from the post-shock temperature and subsequently the radius.

References

1. Astrosat outreach booklet, http://Astrosat.iucaa.in/Astrosat_outreach_book.pdf
2. Astrosat handbook, http://Astrosat.iucaa.in/~Astrosat/Astrosat_handbook_ver1.6.pdf
3. Rao, V. Koteswara, et al. "The Scientific Objectives of the Astrosat Mission of ISRO." Acta Astronautica 65.1-2 (2009): 6-17.
4. Yadav, J. S., P. C. Agrawal, et al. "Large Area X-ray Proportional Counter (LAXPC) Instrument Onboard Astrosat." Space Telescopes and Instrumentation 2016: Ultraviolet to Gamma Ray (2016).
5. Agrawal, P. C., J. S. Yadav, et al. "Large Area X-Ray Proportional Counter (LAXPC) Instrument on Astrosat and Some Preliminary Results from Its Performance in the Orbit." Journal of Astrophysics and Astronomy 38.2 (2017).
6. Singh, Kulinder Pal, Gordon C. Stewart et al. "In-orbit Performance of SXT aboard Astrosat." Space Telescopes and Instrumentation 2016: Ultraviolet to Gamma Ray (2016).
7. Exploring the X-ray Universe (Charles & Seward; CUP)
8. X-ray Binaries (Lewin et al; CUP); 3 rd ed. Lewin & v.d.Klis (astro-ph)
9. Yi, Insu, & Ethan T. Vishniac. "The Hard X-ray Emission Spectra from Accretion Columns in Intermediate Polars." The Astrophysical Journal 435 (1994): 829. Print.
10. Beuermann, K., Th. E. Harrison, et al. "An HST Parallax of the Distant Cataclysmic Variable V1223 Sgr, Its system Parameters, And accretion rate." Astronomy & Astrophysics 419.1 (2004): 291-99. Print.
11. Ezuka, H. & Ishida, M., “Iron Line Diagnostics of the Post shock Hot Plasma in Magnetic Cataclysmic Variables Observed with ASCA”, ApJ Supp., (1999): 120, 277
12. Mukai, K, et al. “Two Types of X-Ray Spectra in Cataclysmic Variables”, ApJL, L77 (2003)